Research Article

Najmeh Alsadat Abtahi, Seyed Morteza Naghib*, Fatemeh Haghiralsadat*, Javad Zavar Reza, Fatemeh Hakimian*, Fatemeh Yazdian, and Davood Tofighi

Smart stimuli-responsive biofunctionalized niosomal nanocarriers for programmed release of bioactive compounds into cancer cells *in vitro* and *in vivo*

https://doi.org/10.1515/ntrev-2021-0119
received August 29, 2021; accepted November 3, 2021

Abstract: Cancer treatment is challenging due to late-stage diagnosis, drug resistance and systemic toxicity of chemotherapeutic agents. The formulation of the drug into nanoparticles (NPs) can enhance the treatment efficacy and effectiveness. Therefore, a new cationic niosomal formulation, which contains Tween 80, Tween 60, cholesterol and lysine amino acid as a platform model to enhance transfection efficacy and reach more acceptable stability, and curcumin (Cur) as a biological anticancer drug, are introduced. Here, the authors focused on the design and synthesis of novel lysine-mediated niosomal NPs for the effectual and controlled release of the antitumor agent, Cur, and turned to optimize niosome formulations, concerning the volume of cholesterol and surfactant to implement these anticancer agents, simultaneously. The characterization of NPs s was carried out and the results showed the successful synthesis of Cur-entrapped niosomal NPs with high efficacy, sufficient positive charges and a favorable size (95/33 nm). The *in vitro* studies have been performed to investigate the cytotoxicity, cellular uptake and apoptosis of normal and cancer cells treated by black niosome, free Cur and niosom-loaded Cur. The results showed that implementing agents by niosome caused enhanced cytotoxicity, uptake and anticancer activity in cancer cells in comparison with normal cells. Furthermore, the effect of this nanodrug was surveyed on the 4T1 xenografted Balb/C mouse tumor model. Cur delivery to cancer models caused a higher tumor inhibition rate than in other groups.

Keywords: nanoparticles, noisome, lysine, Tween, curcumin, cancer treatment

*** Corresponding author: Seyed Morteza Naghib,** Nanotechnology Department, School of Advanced Technologies, Iran University of Science and Technology (IUST), P.O. Box 16846-13114, Tehran, Iran, e-mail: Naghib@iust.ac.ir
*** Corresponding author: Fatemeh Haghiralsadat,** Department of Advanced Medical Sciences and Technologies, Medical Nanotechnology and Tissue Engineering Research Center, Yazd Reproductive Sciences Institute, Shahid Sadoughi University of Medical Sciences, Yazd, Iran, e-mail: fhaghirosadat@gmail.com
*** Corresponding author: Fatemeh Hakimian,** Department of Advanced Medical Sciences and Technologies, Medical Nanotechnology and Tissue Engineering Research Center, Yazd Reproductive Sciences Institute, Shahid Sadoughi University of Medical Sciences, Yazd, Iran, e-mail: f.hakimian90@gmail.com
Najmeh Alsadat Abtahi, Javad Zavar Reza: Department of Clinical Biochemistry, Faculty of Medicine International Campus, Shahid Sadoughi University of Medical Science, Yazd, Iran
Fatemeh Yazdian: Department of Life Science Engineering, Faculty of New Science and Technologies, University of Tehran, Tehran, Iran
Davood Tofighi: Department of Psychology, University of New Mexico, Albuquerque, New Mexico, United States of America; Biostatistics, Epidemiology, and Research Design Support (BERD), Clinical and Translational Science Center, University of New Mexico, Albuquerque, New Mexico, United States of America

1 Introduction

The key factor to raise the overall survival rate in most cancers is the surgical removal of the tumor [1,2]. However, surgery establishes several drawbacks such as infection, pain, side effects of the anesthesia, bleeding, *etc*. [3]. Therefore, the survival rate of cancer patients could be improved by applying a combination of drugs and chemotherapy [4,5]. This method may have serious side effects, especially in older women including fatigue, numbness or tingling in the toes and fingers (neuropathy), and nausea [6]. Nanomaterials have attracted much attention in drug delivery [7,8] and biomedicine [9–12] to address this challenge. Multiresponsive materials, biomaterials and NPs can

be regulated for releasing drugs, genes, proteins and bioactive compounds in a target, according to the specific extracellular/cellular stimuli triggered *via* physical, biochemical, biological and chemical changes [13,14]. These smart systems can direct to transformations in the nanocarrier structure/chemistry, establishing a favorable release profile of the drug in a precise place [8,15].

Cur (a polyphenol extracted from *Curcuma longa*) gained tremendous attention due to its biocompatibility, safety and bioactivities like antiviral, antimicrobial, anti-inflammatory and antioxidant activities (for treatment of several chronic diseases such as cancers, neurodegenerative diseases, obesity, liver disease, metabolic syndrome, arthritis and inflammation) [16]. Recently, Cur (diferuloylmethane, *Curcuma longa* L.) has been applied to prevent the growth of human cancer cells, such as multiple myeloma and colorectal cancer [17]. Several studies have demonstrated that Cur can effectively regulate the balance of ROS within the human body, and possesses a regulatory effect on a variety of diseases that occur among the elderly patient population such as Alzheimer's disease [18]. The main mechanism of Cur activity for cancer prevention and anticancer activities is the suppression of the main elements of the onset, metastasis and progression of various cancers [19].

Cur loaded into nanoscaled drug delivery systems (such as liposomes or niosomes) have created a promising type of drug delivery system in order to transfer drugs safely to their targeted sites and decrease adverse effects on healthy tissues [20]. In contrast to liposome as a targeting carrier, which not only lacks stability at various pH values but also has high costs, niosome can improve the desired properties required for a carrier, including drug solubility, drug bioavailability, drug release, biodegradability, biocompatibility and stability when peptide-based drugs are used [21–23]. Niosomes, as nonionic surfactant vesicles, have a lipid bilayer structure that is suitable for delivering different types of pharmaceutical materials like chemotherapeutic agents, hormones, genes, peptides and antigens [24–26].

Recently, the biological and medical application of amino acids has been offered to improve cell penetration efficacy *via* attaching the hyperbranched arginine cores and positively charged lysine. The essential amino acid, L-lysine, that is formed using the fermentation process is not stable for long-term use [27,28]. Thus, L-lysine and its derivatives are usually exploited for food/drug purposes.

In the present study, we synthesized and characterized lysine-mediated niosomal NPs for controlled release of a bioactive compound, Cur, and optimized nanomaterial formulations, in order to reduce the volume of cholesterol and surfactant and enhance the bio/cytocompatibility simultaneously (Figure 1). The combination of Cur and nanoniosomes may be used as a new cancer drug in clinical applications.

2 Material and methods

2.1 Preparation of lysine-grafted niosome-encapsulated Cur

The niosomes containing cholesterol, Tween 80 and Tween 60 surfactants were prepared using the thin-film hydration technique (DaeJung Metals and Chemicals, South Korea). In brief, cholesterol (Sigma-Aldrich, USA) was mixed with 100 µL of chloroform to obtain different molar ratios of the combination (Table 1). About 500 µg of Cur (Sigma-Aldrich, USA) was dissolved in 3,000 µL of methanol (0.17 g/L) and was inserted into the lipids. The solution was added to tween surfactants under agitation conditions. A thin lipid was formed under reduced pressure in a rotary flash evaporator (Heidolph, Germany). The film was hydrated with 3 mL of PBS at 60°C at pH 7.4 and was sonicated for 30 min using a probe sonicator (model UP200St, Hielscher Ultrasonics GmbH, Germany) to decrease the mean size of the vesicle. The zeta potential, particle size, and entrapment efficiency were also determined to further investigate this niosome. Then, L-lysine amino acid solution (0.1 mg/mL) was added to the niosome solution and incubated for 24 h at room temperature. Finally, the sample was centrifuged for 2 min and washed with PBS and Tween 60 (Figure 2).

2.2 Analyzing the encapsulation efficiency

The entrapment efficiency was analyzed through spectroscopic measurements. A ultraviolet spectrophotometer was used to measure the quantities of niosome-encapsulated Cur (model T80+, PG Instruments, United Kingdom) at 429 nm (λ_{max}) [29]. The efficiency of encapsulation was measured as follows:

$$\text{Encapsulation efficiency \%} = \frac{\text{The amount of CURCUMIN encapsulated within niosomes}}{\text{Total amount of CURCUMIN added}} \times 100$$

2.3 Physical characterization of niosomal vesicles

The physical characterization of niosomal vesicles is detailed in the supporting information (SI).

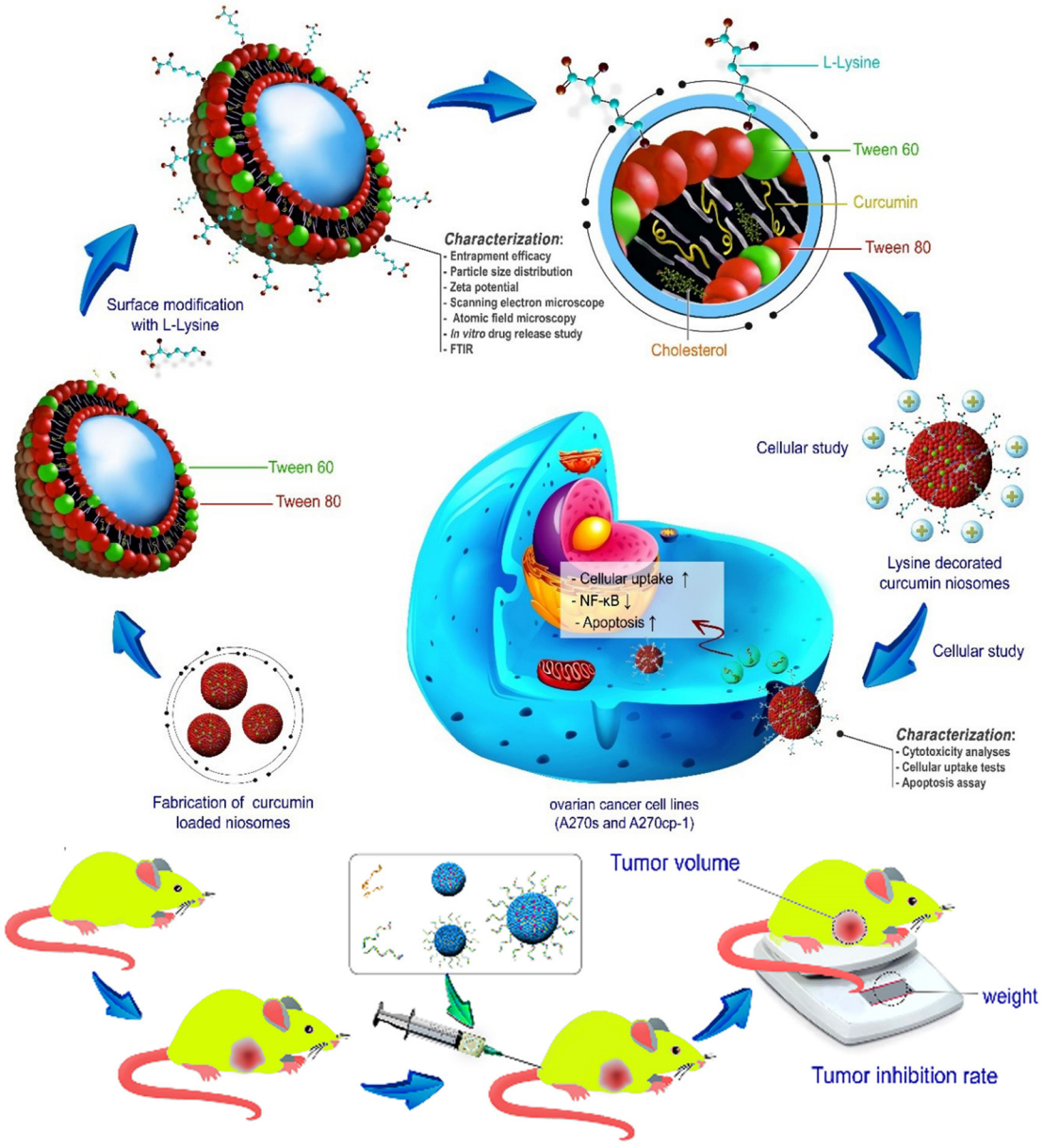

Figure 1: Schematic representation of fabrication and characterization of lysine-mediated niosomal NPs loaded with Cur.

Table 1: The impact of different molar ratios of Tween 80, Tween 60 and cholesterol, on size, zeta potential, entrapment efficiency (EE%), PDI and release percentage (*R*) within the modified niosomes

Code	Tween 80 (%)	Tween 60 (%)	Cholesterol (%)	PDI	EE (%)	Size (nm)	Zeta (mV)
F1	90	0	10	0.272 ± 0.06	59.74 ± 0.003	120 ± 0.012	−23.04 ± 0.01
F2	80	0	20	0.238 ± 0.02	82 ± 0.013	116 ± 0.003	−21.13 ± 0.04
F3	70	0	30	0.221 ± 0.07	73.1 ± 0.16	118 ± 0.023	−24.45 ± 0.06
F4	80	10	10	0.214 ± 0.03	90.1 ± 0.045	111 ± 0.0065	−21.08 ± 0.02
F5	75	15	10	0.202 ± 0.04	96.27 ± 0.086	107 ± 0.054	−18.34 ± 0.09
F6	70	20	10	0.206 ± 0.05	100 ± 0.002	92.01 ± 0.001	−26.92 ± 0.00

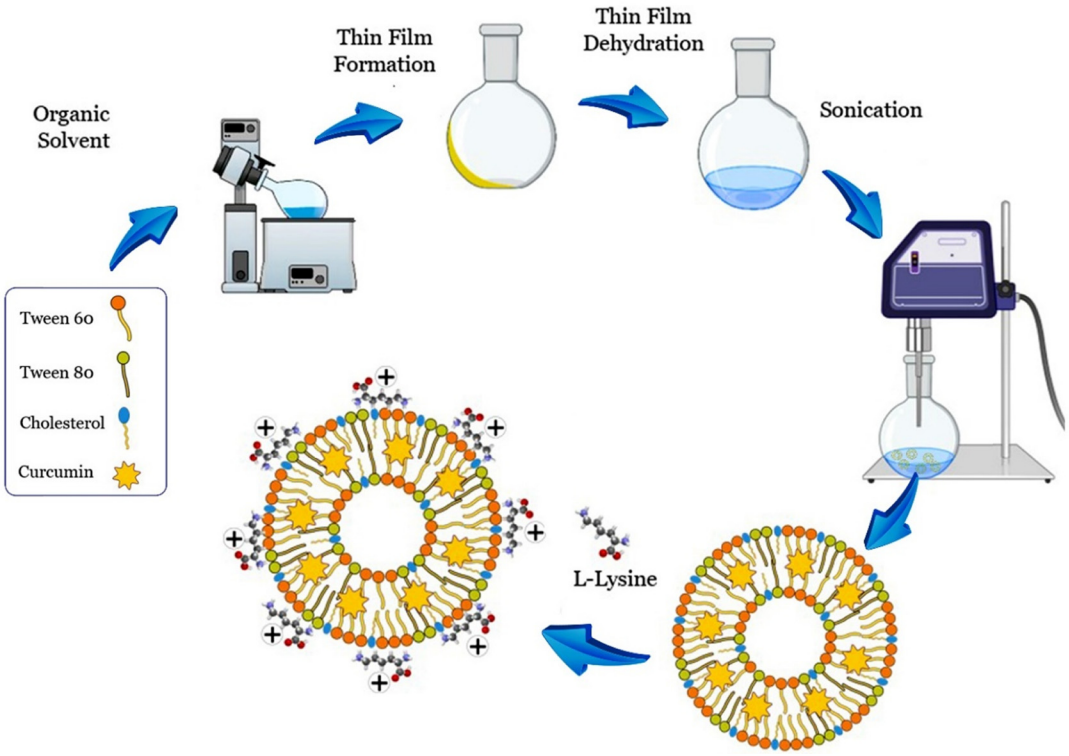

Figure 2: Schematic representation of the synthesis method and preparation of lysine-mediated niosomal NPs loaded with Cur.

2.4 *In vitro* drug release study

The *in vitro* drug release study is detailed in the SI.

2.5 Cell culture, cytotoxicity analysis and cellular uptake of nanoniosomes-loaded Cur

The cell culture, cytotoxicity analysis and cellular uptake of nanoniosomes-loaded Cur are detailed in the SI.

2.6 Cell apoptosis assay

The cell apoptosis assays are detailed in the SI.

2.7 *In vivo* experiments

The *in vivo* experiment protocols are detailed in the SI.

2.8 Statistical analysis

Statistical data are detailed in the SI.

3 Results and discussion

3.1 Effects of surfactants and cholesterol ratios on niosome formulation

In order to control the drug release, vesicle size and entrapment efficiency, different formulations of niosomal NPs were synthesized. In this regard, the concentration of Cur in the system was kept constant and other substances including Tween 80, Tween 60 and cholesterol, were chaged in each formulation (Table 1). According to Table 1, Tween 80 in the absence of Tween 60 shows a significant effect on the Cur entrapment efficacy in niosomes, so that its amount increased from about 60 to 73%. Cur entrapment efficiency was further increased by the addition of Tween 60 surfactant to niosomal Cur formulations, resulting in 100% entrapment efficiency of the designed system (an increase of 10% in F4, and an increase of 20% in F6, respectively). In addition to the effect on the efficiency of Cur loading, Tween 60 surfactant also decreased the mean diameter of niosomes from 111 ± 0.006 to 92.01 ± 0.001 nm, representing a decrease of about 18% in the particle size (PDI was constant in all formulations and zeta potential was relatively small in the negative range). These findings were similar to those

reported by Agarwal *et al.* [30], which showed that increased surfactant hydrophilicity established a bigger vesicle size. Finally, based on high entrapment efficiency, the F6 formulation was selected as the optimal sample for further studies.

3.2 The effect of lysine amino acid in niosomal formulation

Since F6 formulation was chosen as the optimal sample, according to the parameters measured in Table 1, the effect of lysine concentration was also examined in F6, which can be seen in Table 2. The addition of lysine led to a decrease in PDI, which reached 0.182 for the F7 formulation compared to 0.206 for F6, as expected. Also, the zeta potential was significantly reduced when the lysine concentration in F9 reached 10^{-1} mol/mL (from −26 mV for F9 to −5 mV for F6), which could be related to close relationship with the lysine charge.

On the other hand, there was no considerable change in the vesicle size of niosomes added to the lysine solution. Therefore, niosomal formulation containing Tween 80/Tween 60/cholesterol in a molar ratio of 70:20:10, and lysine at a concentration of 10^{-1} mol/mL (F9) were used. Therefore, all the parameters listed in Table 2, including the controlled release of Cur, entrapment efficiency, small diameter and enhanced transfection effectiveness were suitable for this sample.

3.3 Characterization of modified niosome NPs

SEM and CryoTEM images of the modified nanocarriers are depicted in Figure 3a and b. As shown in the figures, the lysine-grafted niosomal NPs were spherical and round with a smooth surface, as well as there was not considerable aggregation in this formulation. Atomic forces microscopy (AFM) analysis was used to investigate the shape and distribution of the particles, as shown in Figure 3c. AFM images showed a spherical and multilamellar structure of the modified carrier (F9). There was no evidence for aggregation of niosomal NPs after one day of storage at 4°C, which was predictable according to the results obtained from Tables 1 and 2 because the zeta potential was significantly reduced from −26 mV for F6 to −5 mV for F9 (80% reduction), after the addition of lysine to niosomes. Release profiles of nanoniosomes and lysine-modified

Table 2: Effect of the concentration of lysine on PDI, size, entrapment efficacy (EE%), zeta potential and release percentage (R) in the modified niosomes

Code	Tween 80 (%)	Tween 60 (%)	Cholesterol (%)	Lysine (mol/mL)	PDI	EE (%)	Size (nm)	Zeta (mV)
F7	70	20	10	10^{-3}	0.182 ± 0.02	99.35 ± 0.085	94.02 ± 0.034	−18.41 ± 0.02
F8	70	20	10	10^{-2}	0.178 ± 0.06	98.24 ± 0.016	98.16 ± 0.023	−10.6 ± 0.45
F9	70	20	10	10^{-1}	0.164 ± 0.059	100.001 ± 0.653	95.33 ± 0.034	−5.23 ± 0.054

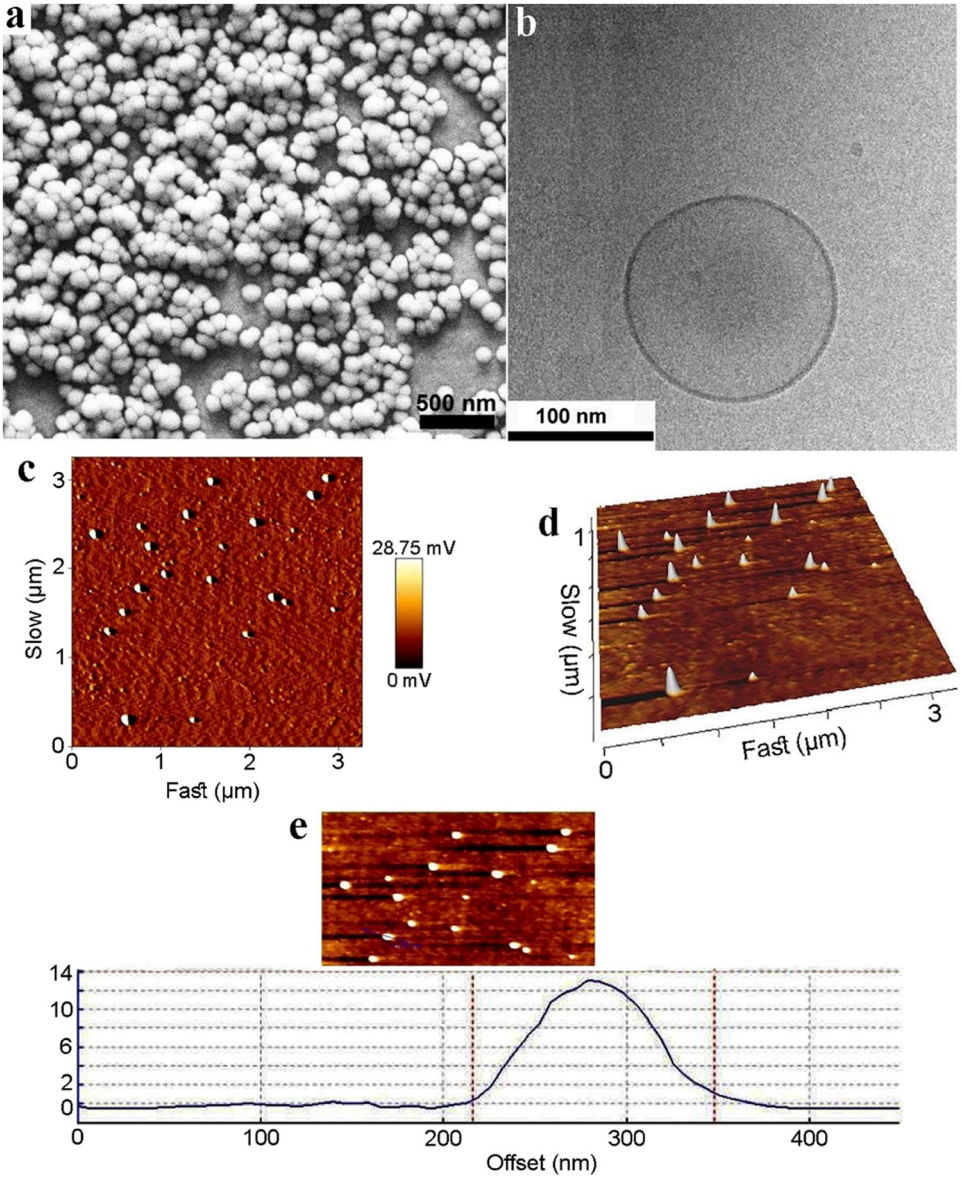

Figure 3: (a) SEM image of the modified niosomal NPs; (b) cryo-TEM image of the modified niosomal NPs; (c–e) 2D, 3D, and line analysis of the AFM image of the modified niosomal NPs, respectively.

nanoniosomes from optimal formulations (F6 and F9) in PBS at a pH of 7.4 and 37°C is shown in Figure 4a and b. According to the obtained 3D images, approximately 32.33% of the loaded drug in nanoniosomes, and 28.23% of the loaded drug in modified nanoniosomes were released after 72 h. The Cur release profile in both niosomes was biphasic with a primary quick release period, followed by a slower release. Physical stability of the modified nanoniosomes after storing for 15, 30, 45, and 60 days was assessed by measuring the vesicle size, zeta potential and entrapment efficiency (Figure 4c) at 4°C. As can be seen, the parameters mentioned above had a steady trend during these 2 months, and their changes during this period of time were relatively low (p-value of less than 0.05). To confirm the loaded Cur in nanoniosomes, Fourier-transform infrared spectroscopy (FTIR) examinations were established. Figure 4d demonstrates the FTIR spectra of Cur, blank noisome, Cur loaded in noisome and Cur loaded in noisome modified by lysine. The bands of Cur shown in the figure were C–H out-of-plane bending vibrations in 800–600/cm, C=O stretch at 1,152/cm, aromatic ring C=C stretching at 1,506/cm, and O–H and C–H stretching at 3,507/cm. The FTIR pattern of the blank niosome showed various characteristic peaks of ingredients in the range 3,500–1,115/cm; The peak at 3,435/cm was attributed to Tween-60 and cholesterol (O–H stretching

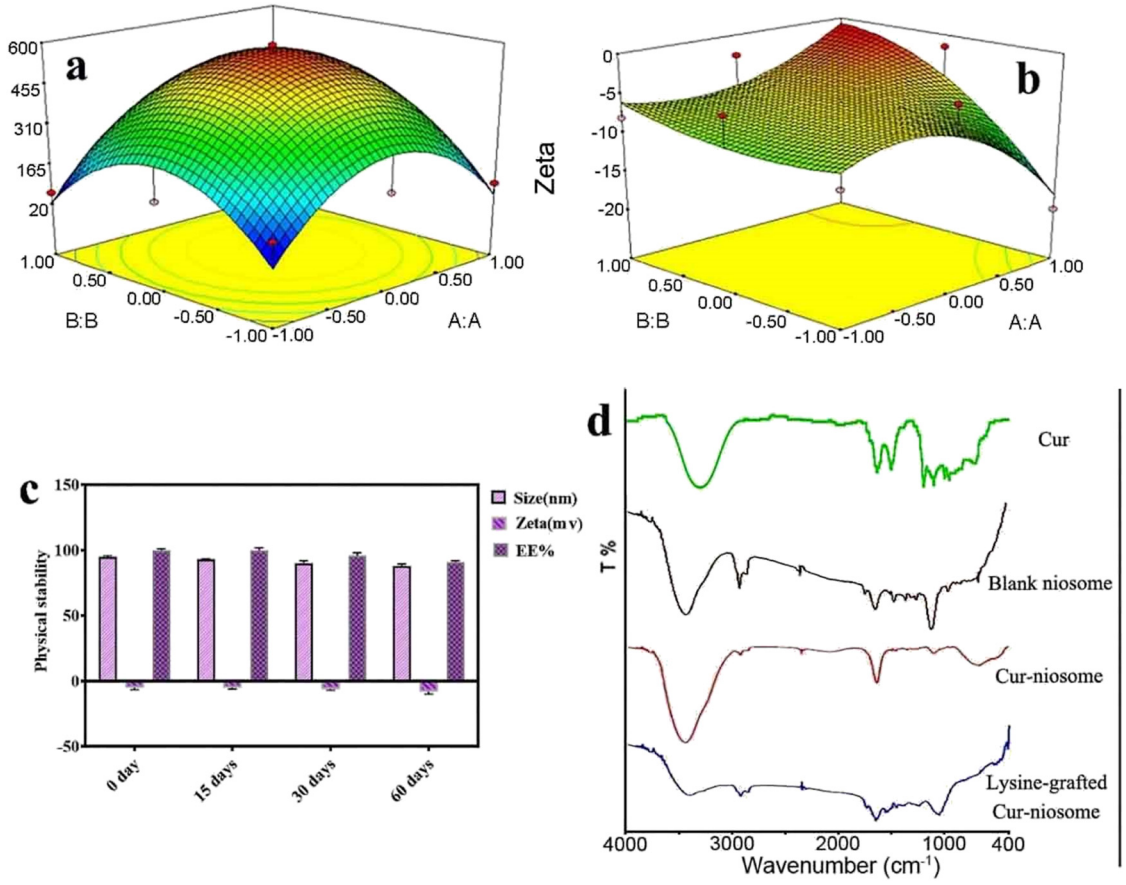

Figure 4: The response surface plot of the (a) droplet size and (b) zeta potential. (c) Physical stability of the modified niosomal NPs during two months. (d) FTIR spectra of Cur, blank noisome, Cur loaded in noisome NPs, and lysine-grafted Cur-niosomal NPs.

in phenols and N–H stretching in 2°-amines). The C–O stretch belonged to Tween-60 that occurred at 1,148/cm. C═O exhibited a robust absorption band at 1642.15/cm, owing to the stretch vibration of C–O in Tween 60. The results of FTIR analysis of free Cur presented the C–H out-of-plane bending vibrations in the region 800–600/cm, C═O stretching at 1,152/cm, aromatic ring C═C stretching at 1,506/cm, and O–H and C–H stretching at 3,507/cm. In comparison with the unmodified noisomes, the broader bands at 3,500 and 500–900/cm, and the sharper band at 1,600/cm, confirmed the entrapment of the drug into the carriers. The presence of the entrapped Cur in nanoniosome formulations was confirmed by FTIR analysis.

3.4 *In vitro* Cur release from the modified noisome NPs

Investigation of *in vitro* release of Cur was carried out by the dialysis approach. The results of 72 h release profiles of Cur loaded in modified noisomes, from F9 in both plasma and PBS at temperatures of 25, 37, and 42°C at pH 7.4 and 5.5, are shown in Figure 5. In Figure 5a–d, it is quite obvious that the rate of drug release increases with increasing temperature from 25 to 42°C. After 72 h in plasma, 14.45, 18.23, and 20.34% of the loaded drug and 12.45, 14.23, and 16.34% of the loaded drug were released at pH 7.4 and 5.5, respectively, which indicated that an increase in pH increased the drug release rate. The release rate in PBS at pH 7.4 was significantly different from the obtained data in plasma, so that drug release increased from 20.34 to 30.34% at 25°C (an increase of almost 50%). The same conditions were used to assess drug release at pH 5.5. The cumulative release profile of the drug was obviously biphasic and the early fast release phase was followed by a slower release period. In addition, the Cur release rate of noisomes was compared to that of niosomes modified by lysine, as indicated in Figure 5e. Lysine was able to reduce the release rate of Cur by about 17% compared to the blank niosomes, demonstrating the effectiveness of the modified nanocarriers.

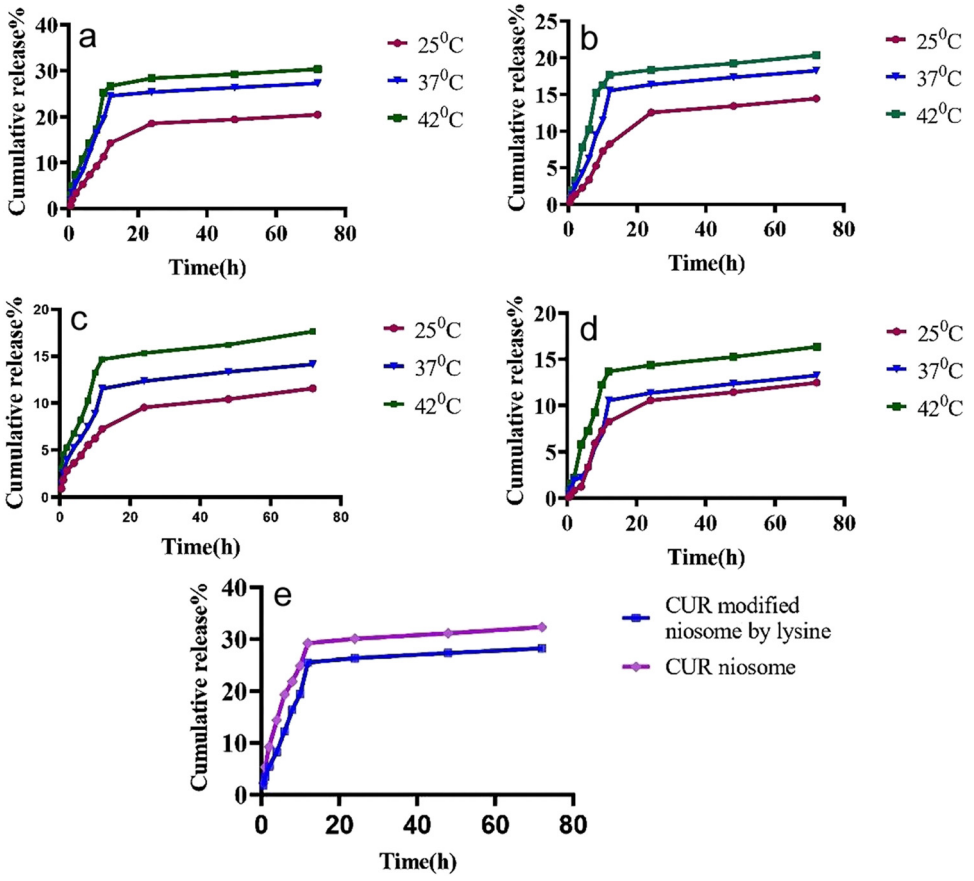

Figure 5: (a and b) *In vitro* release of the modified niosomal NPs in PBS at pH 7.4 and 5.5; (c and d) *in vitro* release of the modified niosomal NPs in plasma at pH 7.4 and 5.5; (e) the release rate of DOTAB-mediated niosomal NPs and lysine-mediated niosomal NPs in PBS at pH 7.4 for 72 h.

As a stimuli-triggered material/polymer-encapsulated drug/therapeutic agent is established for programmable and on-demand drug delivery, its release can be started with changes in the structure such as charge switching, surface layers de-shedding and degradation of materials [31]. Moreover, breaking of a bond can be established that starts the release of drugs that are covalently immobilized to the functional groups of materials [32]. A smart pH-responsive system can be used for the site-specific release of drugs *via* altering the solubility of the nanocarrier or *via* cleaving a pH-responsive bond [33]. When oral administration is used for the delivery of a drug to the tumor (colon), this system is very useful because the pH of the stomach is lower than that of the colon, which helps deliver the drug in the colon. The temperature of tumor tissues are higher than that of normal tissues [34], which can be applied for stimuli-sensitive tumor-targeted drug delivery.

3.5 Optimization of lysine volume and concentration on the zeta potential and nanoparticle size

The results of the statistical analysis of volume and concentration of lysine on the zeta potential and nanoparticle size are shown in Table 3. For this purpose, both the maximum value of the zeta potential and the minimum value of the nanoparticle size were considered under optimal conditions. The results were consistent with the second-order polynomial equation. The number of regression coefficients was measured. The fitted equation (based on the coded values) for the nanoparticle size and zeta potential ($R^2 = 0.91$ and $R^2 = 0.75$, respectively) is

$$\text{Size of nanoparticle} = +561.13 + 40.85 \times A + 25.28 \times B + 27.92 \times A \times B - 258.01 \times A^2 - 233.91 \times B^2, \quad (1)$$

Table 3: Statistical design for the optimization of volume and concentration of lysine

Run	Lysine volume	Lysine concentration
1	−1	−1
2	1	−1
3	−1	1
4	1	1
5	−1	0
6	1	0
7	0	−1
8	0	1
10	0	0
11	0	0
12	0	0
13	0	0

$$\begin{aligned}\text{Zeta potential} = {} & -5.61 + 1.58 \times A + 0.30 \times B \\ & + 3.84 \times A \times B - 1.35 \times A^2 \\ & - 1.27 \times B^2 + 4.54 \times A^2 \times B \\ & - 2.74 \times A \times B^2,\end{aligned} \tag{2}$$

where A and B are the volume and concentration of lysine, respectively. One constant and two quadratic terms were recorded by the regression model coefficients (equations (1) and (2)). The importance of each coefficient was demonstrated with p-values. The obtained determination coefficient ($R^2 = 0.91$) showed that 91% variability within the response could be described with this model. Moreover, the obtained zeta potential (75%) was in good agreement with the proposed model (equation (2)). The optimal values of the variables from the quadratic model

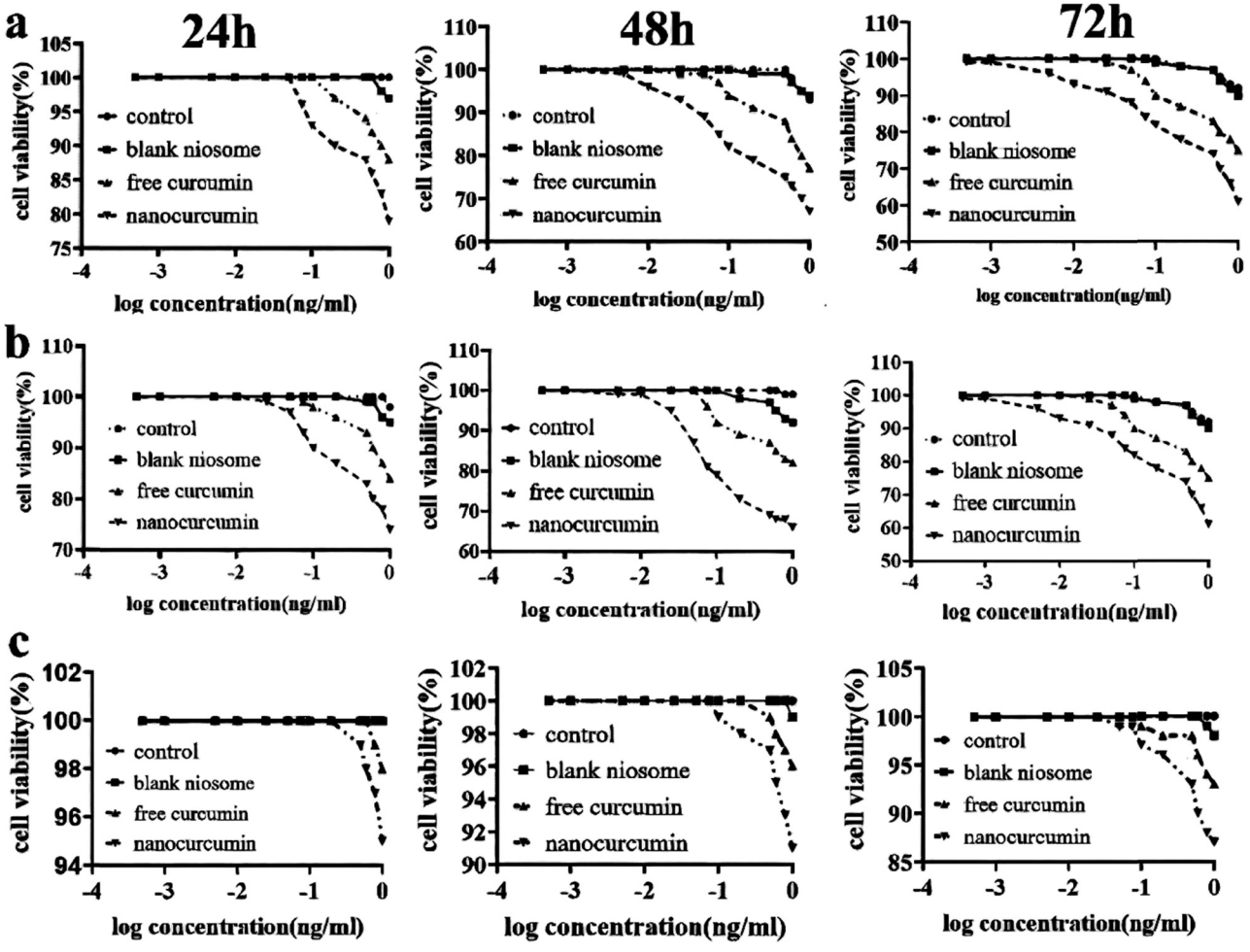

Figure 6: (a) The cell viability 2,5-diphenyl-2H-tetrazolium bromide (MTT) analysis of the modified niosomal NPs in A270CP-1, (b) MTT analysis of the modified niosomal NPs in A270S cells, and (c) MTT analysis of the modified niosomal NPs in MCF10-A cells. The assays were carried out three times to obtain the mean ± standard deviations.

differentiation were obtained. The predicted optimum nanoparticle size and zeta potential corresponding to these values were about 163.27 nm and −0.71, respectively. The model accuracy was confirmed to predict the optimal value. Further experiments were carried out in triplicates, using the enhanced essential aspects (codes 1 and 1 for *A* and *B*). The regression equations were graphically represented as 3D plots, which demonstrated the interaction of the variables (Figure 4a and b). The plots of elliptical contour indicated that the interactions were essential to enhance the optimum conditions.

3.6 Cytotoxicity assays

Cytotoxicity of niosome, the niosome loaded with Cur, and the modified niosome loaded with Cur against MCF10-A cells and the ovarian cancer cell lines, A270s and A270cp-1, were evaluated by MTT assays after 24, 48, and 72 h incubation, and they were compared with untreated cells as a control sample. From Figure 6, it is evident that cell viability decreased progressively once the cells were treated with Cur and nanocarriers. The modified nanocarriers presented more reduction in cell viability of tumor cells in lower dosages. The IC50 value for the modified niosome was between 0.035 and 0.068 μM, compared to that for free Cur, which was 0.08 to 0.135 μM in cancer cells. The results showed that IC50 was between 0.0513 and 0.0827 μM; however, it changed between 0.112 and 0.201 μM for free Cur. The assay demonstrated that the IC50 value in cancer cells was lower than that in normal cells (~1.5-fold) for free Cur and the modified niosome as well as lower in the niosomal form than that in the free form in all cells. Furthermore, a higher number of viable normal cells were observed for the same concentration of the modified NPs. These findings confirmed that Cur in niosomal and free forms imposed low cytotoxicity over MCF-10A normal cells (Figure 7).

3.7 Intracellular uptake studies

After formulation and characterization of the modified nanoniosomes, we evaluated the ability of these niosomes to be endocytosed by cells. Figures 8 and 9 show an entire panel of the fluorescence microscope images of different cancer cell lines, A270cp-1 and A270s cell lines, incubated with the modified nanocarriers for 4 h. Our results depicted the robust uptake of the nanoniosomes in cancer cell lines. Control cells without any Cur or niosome treatment did not show any fluorescence (data not shown).

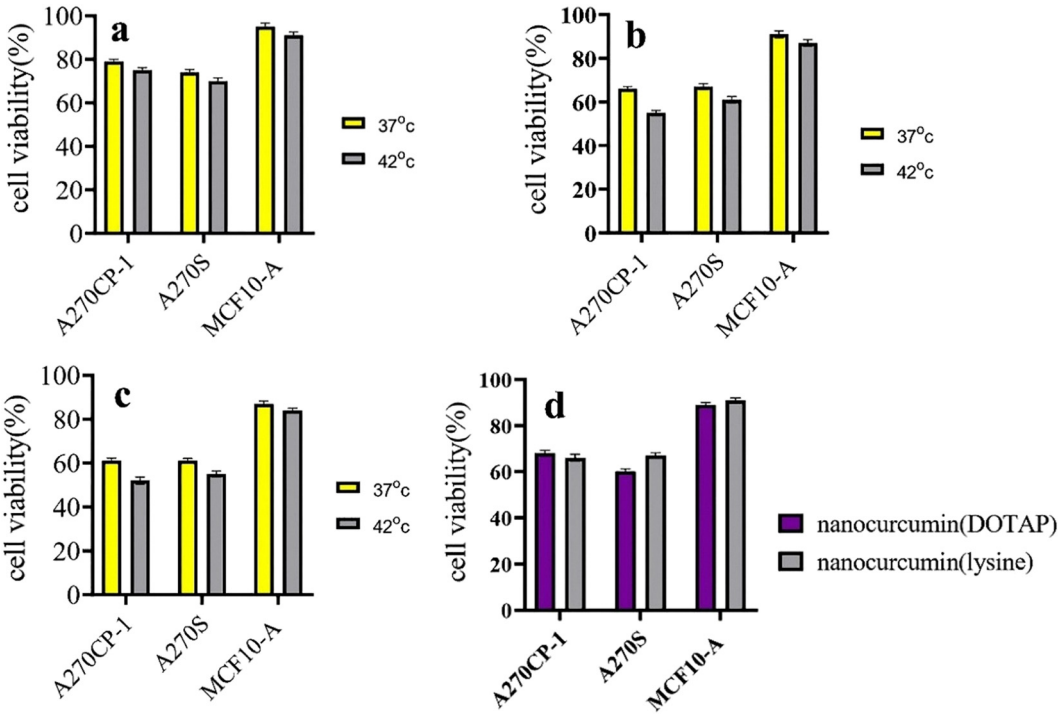

Figure 7: (a) The cell viability analysis of the modified niosomal NPs in cancerous and normal cells at 37 and 42°C for 24 h. (b) The cell viability analysis of the modified niosomal NPs in cancerous and normal cells at 37 and 42°C for 48 h. (c) The cell viability analysis of the modified niosomal NPs in cancerous and normal cells at 37 and 42°C for 72 h. (d) The cell viability analysis of the lysine-mediated niosomal NPs and the DOTAP-mediated niosomal NPs in cancerous and normal cells at 37°C for 48 h.

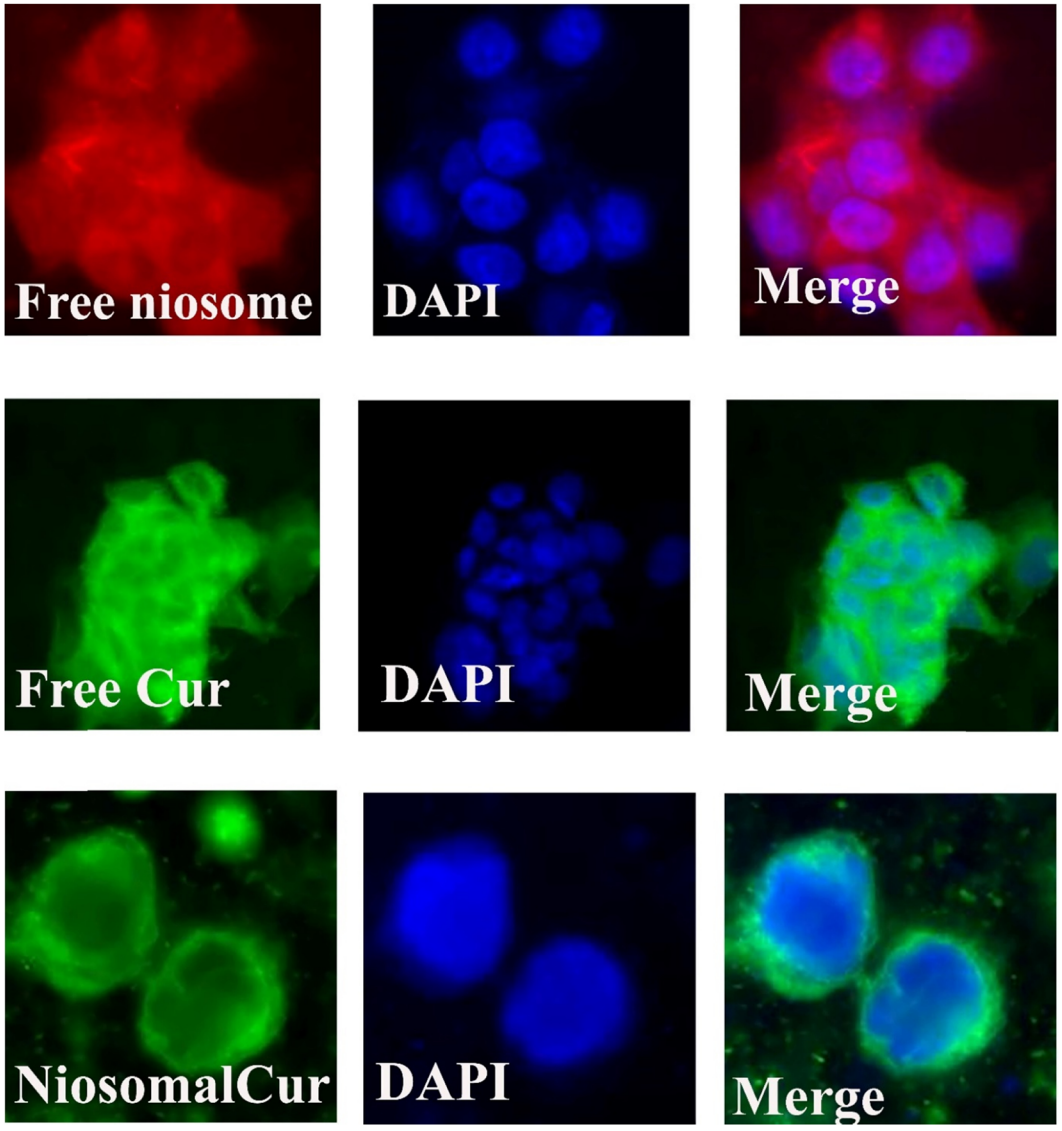

Figure 8: Cellular uptake images of A270cp-1 incubated with the modified niosomal NPs for 4 h.

The cells incubated with the modified nanocarriers exhibited greater green intensity compared to the cells treated with DOTAP, demonstrating rapid internalization and accumulation of the modified nanoniosone-loaded Cur in cancer cells. These results indicated that Cur inserted the cancerous cells at a much higher rate than that in healthy cells. The findings confirmed the obtained results from cytotoxicity tests.

3.8 Apoptosis assay

Quantitative apoptotic activity measurements were performed *via* flow cytometry analysis. The statistically significant apoptotic activities of the modified nanocarriers were compared with free Cur solution in cancer cells ($p < 0.05$). The flow cytometry analysis indicated that the cell apoptosis for the modified nanocarriers was considerably higher than that for free Cur as shown in Figure 10a ($p < 0.05$).

3.9 Gene expression

To validate the downstream impact of Cur gene silencing efficiency, expression levels of Nf-κB and P53 were used to analyze the entrapped drug efficiency. Nf-κB inhibits cell death through mitochondrial apoptosis pathways. This research utilized the qRT-PCR techniques for detecting the P53 and Nf-κB expression, after the

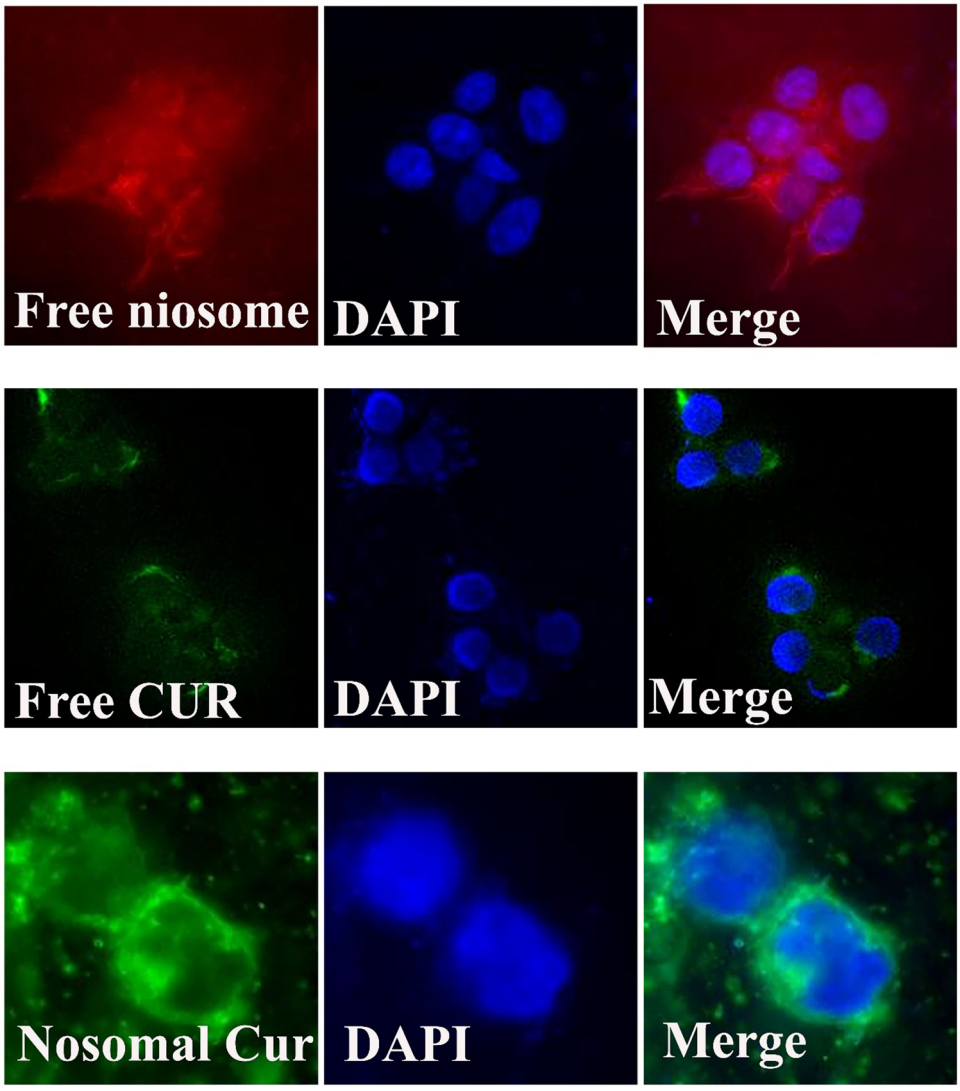

Figure 9: Cellular uptake images of A270s incubated with the modified niosomal NPs for 4 h.

restoration by cancer cell lines at the transcription level. After treatment of cells with free Cur and the modified nanocarriers, the relative expression of NF-κB and P53 genes in the cells was evaluated. According to Figure 10b and c, the expression of Nf-κB and P53 on the cancer cells treated with a solution containing Cur did not exhibit any significant differences in comparison with the control cells. The results of NF-κB and P53 gene expression showed that free Cur caused low NF-κB expression and high P53 expression when compared to the control cells. Moreover, the change in the expression of the above genes in the cells treated with the modified nanocarriers was more considerable compared to the free drug. Our results confirmed the previous observations.

The present standard care for cancer is chemotherapy and/or surgery that have several side effects in patients. Therefore, it is necessary to develop new approaches for reducing the side effects. In this regard, Cur has received much attention as an alternative for conventional treatments. It has been shown that natural compounds possess chemopreventive and/or anticancer activities with minimum side effects [35]. Cur, a natural diphenol extracted from *Curcuma longa* ground rhizomes, has some potential beneficial biological features such as chemoprevention and anticancer features [36]. Despite these excellent effects, the use of Cur has been limited because of its low therapeutic index and poor aqueous solubility. The best way these problems were solved over the past 30 years was the use of a vesicular nanocarrier like niosome. Niosomes have been utilized successfully as a drug delivery system for solving some main biopharmaceutical issues. They are vesicular systems that can entrap the hydrophilic drug and

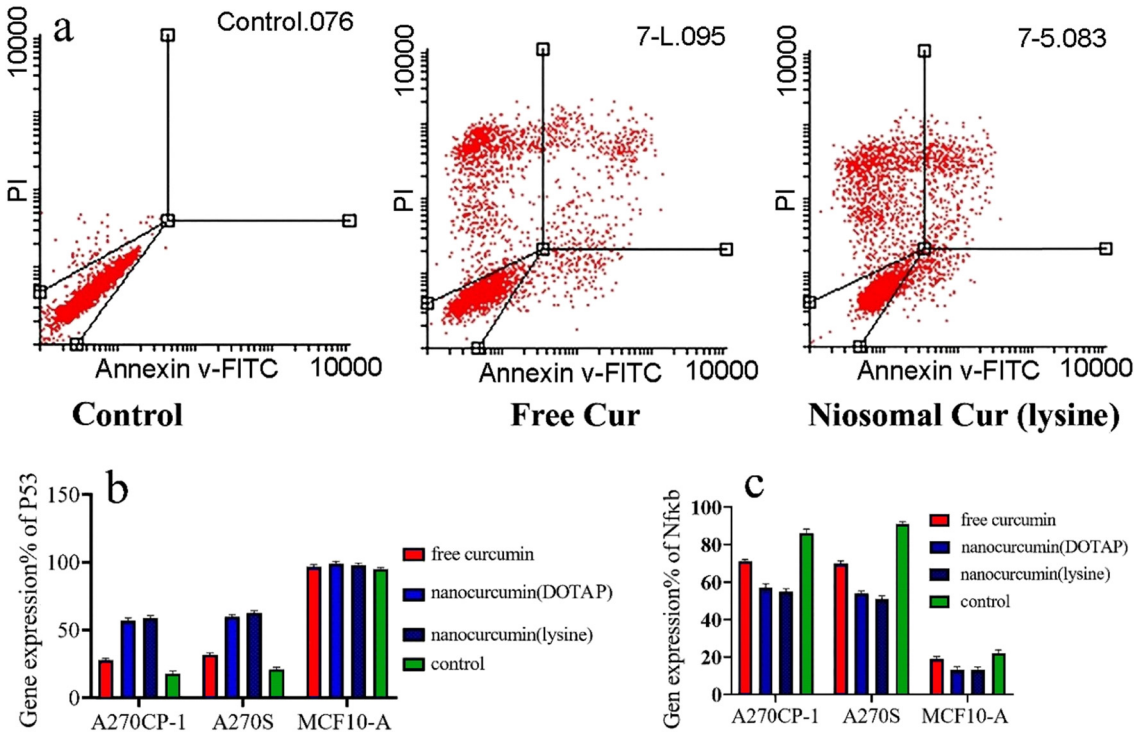

Figure 10: (a) Apoptosis assay by flow cytometry, after treating the cells for 48 h. (b and c) Real-time PCR quantitative analysis of p53 and Nf-κB expression after the treatment with different formulations for 48 h.

hydrophobic drugs, simultaneously. Therefore, hydrophobic and hydrophilic drugs are combined into niosomes [37]. The formation of niosomes requires an amphiphilic molecule including two main parts: a polar head or a hydrophilic group and a nonpolar or a hydrophobic tail as the structure of the surfactant molecules. Cholesterol in niosomes can considerably change the membrane permeability, fluidity, vesicle stability, niosomes size, and entrapment efficiency [38,39]. Here, the charged molecules were added into niosome formulation to improve the vesicle electrostatic stability and to increase the encapsulation efficiency. These molecules can attach to the cell membrane because, in most cells, there is a negative charge on the cell membrane. Afterward, the charged nanocarriers enter the target cell by endocytosis [40,41]. DOTAP is the best choice used in this regard. Although DOTAP is cheap and efficient in both *in vivo* and *in vitro* delivery [42], it has been limited due to its toxicity and susceptibility to protein-induced aggregation in blood [43]. So, altering the pathway is necessary as it increases the niosome charge without side effects. Lysine is an essential amino acid that is important for normal growth and muscle turnover and helps transport fats across cells. Lysine with its lysyl side chain ($((CH_2)_4NH_2)$) is a basic, positively charged, and the polar amino acid at pH 7. It plays a vital role in the structure as an amphipathic and hydrophobic part of the side chain. Moreover, it is involved in the salt bridge, where it is paired with the negatively charged atoms (anion or carboxylate group) to create hydrogen bonds [44]. These special properties make lysine amino acid a better choice than DOTAP. In this work, we created a new cationic niosomal formulation modified by lysine amino acid that encapsulated Cur. PDI%, EE%, size, and zeta potential were evaluated at two levels. First, the vesicular system was made from tween 80 (nonionic surfactant) and cholesterol. We obtained perfect results after the addition of Tween 60, which increased entrapment efficiency and vesicle zeta potential and decreased PDI and vesicle size. Tween 80 was used as the safest surfactant; however, a slight amount of Tween 60 was also essential for the effective results. Second, the vesicular systems were analyzed after the addition of lysine at different concentrations. The results showed improved stability, decreased mean size diameter, enhanced drug encapsulation and increased mean zeta potential. So, lysine like DOTAP could functionalize the nanocarriers for amending cell attachment, encapsulation efficiency and controlled release behavior of the modified nanoniosemes, and reducing side effects through a reduction in the cholesterol content. It also reduces the PDI related to the additional reciprocal repel force, within the particles with the same sign charge in the suspension system. Introducing a charge over

the vesicle surface is essential to prevent the aggregation of vesicular systems. Furthermore, in sharp contrast to DOTAP, lysine is an essential amino acid in the body. On the niosome surface, lysine is changed to safer particles that make it more positive than DOTAP. Keeping the niosomal suspension at 4°C for 60 days, there was no sharp changes in comparison with the fresh specimens, based on encapsulation efficiency, zeta potential, and vesicle size of the improved formulation. This result indicates that the novel niosomal nanocarriers modified by lysine can decrease several drawbacks such as niosome instability, niosome aggregation, drug leakage and drug fusion. Based on the release rate of the nanocarriers, it is found that the cumulative release profile of the drug is biphasic. The diffusion mechanism controlled the rate of release quickly (concentration gradient of the drug between the buffer and niosome), while the slow drug release phase was sought by the inner layer [36]. We also investigated the MTT of free Cur and the modified carriers on A270s and A270cp-1 cells (Figures 6 and 7). The results showed higher cytotoxicity effects. The examination of Cur demonstrated that free and niosomal Cur induces cell cycle arrest or apoptosis and most importantly downregulated nuclear factor kappa B (NF-κB) expression in various human cancer cell lines [45,46]. Apoptotic activity measurements by flow cytometry showed that there were statistically significant results for lysine-mediated nanocarriers, in comparison with the apoptotic activity of the niosomal Cur and free Cur ($p < 0.05$).

3.10 Assessment of the *in vivo* tumor inhibition abilities

The anticancer effects of the control, free Cur, niosomal Cur and biofunctionalized nanocarrier loaded with Cur were evaluated by 4T1 xenografted Balb/C mice. To administer different formulations, the mice were injected with free Cur, niosomal Cur (DOTAP), biofunctionalized nanocarrier loaded with Cur, and normal saline on days 0, 3, 6, 9, and 12 after the tumor reached 100 mm^3. On day 21, the mice were sacrificed, the tumor tissues were detached and the mice volumes were measured. Compared to the control (2,320 ± 200 mm^3), the group administered with free Cur (1,180 ± 100 mm^3) depicted smaller tumor tissues on day 21. The tumor tissues of the group administered with niosomal Cur (DOTAP) (880 ± 50 mm^3) and niosomal Cur modified by lysine (810 ± 100 mm^3) were

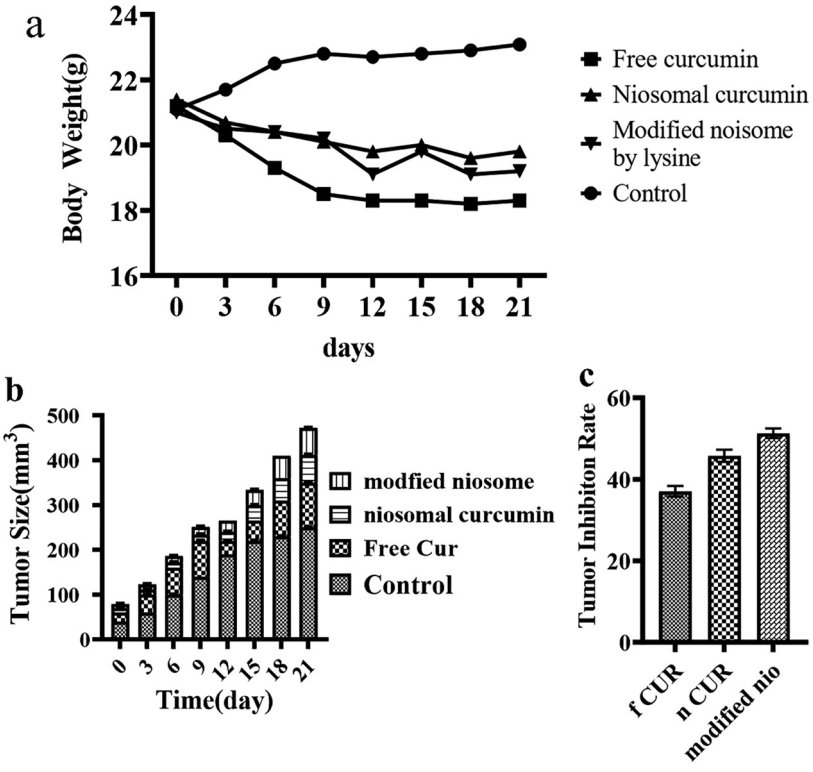

Figure 11: (a) Influence of different formulations on the mouse weight, evaluated every 3 days. (b) The effects of the formulations on the tumor size (mm^3). (c) Tumor inhibition rate (f: free; n: noisome; nio: niosome). Data were exhibited as the mean ± SD and $p < 0.05$ was considered a significant statistical difference.

Table 4: Bodyweight of mice that received different therapies

Time (days)	Control	Free Cur	Niosomal Cur	Modified noisome by lysine
0	21.1	21.2	20.1	20
3	21.7	20.3 ± 0.3	20.7	20.5
6	22.5 ± 0.1	19.3	20.4	20.4 ± 0.01
9	22.8	18.5	20.1	20.2
12	22.7	18.3 ± 0.3	19.8 ± 0.1	19.1
15	22.8 ± 0.1	18.3	20	19.8 ± .01
18	22.9	18.2 ± 0.1	19.6 ± 0.1	19.1
21	23 ± 0.2	18.3	19.8 ± 0.1	19.2 ± 0.1

even smaller than that of the group administered with free Cur. Nevertheless, the group treated with the biofunctionalized niosomal Cur depicted the smallest volume among all treated groups (Figure 11a). Based on Figure 11b, changes in free Cur, niosomal Cur and the biofunctionalized nanocarrier loaded with Cur are triggered by the constant growth inhibition, established by the mentioned formulations. The results suggested that the modified niosomal Cur could enhance the tumor inhibition potential and offer advanced therapeutic influence more than DOTAP-mediated niosomal Cur and free Cur.

After every administration, to evaluate the toxic effects of different formulations, the changes were monitored in the mice weight, every 3 days (Figure 11c and Table 4). The control group depicted an increase in body weight while, in other groups, the weight was marginally decreased on day 21. According to Figure 11c, a quick weight loss is identified in the free Cur-treated mice in comparison with other groups after 6 days. The results showed that the amended nisomal Cur did not enhance the toxic effects in comparison with the niosomal Cur.

miRNA-34a, a known tumor suppressor, is involved in various processes in a cell. miRNA-34a regulation influenced by the p53 gene and Sirt1 was depicted as one of the miR-34a targets, whose Sirt1 expression was related to P53. An increase in miRNA-34a levels establishes a reduction in Sirt1 bioactivity and stimulates P53 bioactivity. Moreover, one of the approaches inducing differentiation in the cells by miRNA-34a is the expression regulation of Wnt1. Wnt1 was depicted as the target of miRNA-34a. Decrease of Wnt1 stimulates cells differentiation [47]. Furthermore, previous findings demonstrated that miRNA-34a reduced the level of EGFR and MMP7 expression in tumor cells by triggering enzymatic cascades downstream of the EGFR signaling pathway, including PI3K.

Many potent chemopreventives were extracted from plants; however, Cur exhibited one of the most studied phytochemicals [48]. Recent research studies demonstrated that Cur can be a potent antiarthritic, antithrombotic, antiatherosclerotic, hepatoprotective, antidiabetic, antiangiogenic, antimetastatic, antiproliferative, anti-inflammatory and antioxidant agent in *in vitro* and *in vivo* [49]. Many surveys demonstrated that Cur could induce apoptosis in cancer cells *via* inhibition of different intracellular transcription factors and secondary messengers like NF-kB, AP-1, c-Jun, and the JAK-STAT pathway [8]. Moreover, Cur had considerable potential for inhibiting carcinogenesis established by biochemical carcinogens [50]. Cur also enhances the level of endogenous antioxidants through the Nrf2 pathway to boost body defense against ROS [8]. In spite of these benefits, Cur possessed poor water solubility and so it exhibited solubility limited bioavailability (class II drug in the Biopharmaceutics Classification System) [48]. To address this challenge, promising modified niosomal NPs were proposed in this research that could increase bioavailability through enhancing solubility.

4 Conclusion

Niosomes are nonionic surfactant vesicular systems that can be considered as efficient and emerging materials for drug delivery applications. High efficiency and minimum toxicity are the targets for designing a new formula. Our findings suggested a novel lysine-mediated niosomal formulation that could cover these goals. The encapsulation efficiency of the drug and MTT test was extremely successful. The obtained results indicated that the novel formula was effective for killing cancer cells *in vitro* and *in vivo*.

Funding information: The authors state no funding involved.

Author contributions: All authors have accepted responsibility for the entire content of this manuscript and approved its submission.

Conflict of interest: The authors state no conflict of interest.

References

[1] Sternby Eilard M, Lundgren L, Cahlin C, Strandell A, Svanberg T, Sandström P. Surgical treatment for gallbladder cancer–a systematic literature review. Scand J Gastroenterol. 2017;52(5):505–14.

[2] Rahimzadeh Z, Naghib SM, Askari E, Molaabasi F, Sadr A, Zare Y, et al. A rapid nanobiosensing platform based on herceptin-conjugated graphene for ultrasensitive detection of circulating tumor cells in early breast cancer. Nanotechnol Rev. 2021;10(1):744–53.

[3] Sánchez-Elvira LA, Martínez SB, del Toro Gil L, Tello VG. Postoperative management in the Intensive Care Unit of head and neck surgery patients. Medicina Intensiva (Engl Ed). 2020;44(1):46–53.

[4] Zhao W, Cong Y, Li H-M, Li S, Shen Y, Qi Q, et al. Challenges and potential for improving the druggability of podophyllotoxin-derived drugs in cancer chemotherapy. Nat Product Rep. 2021;38(3):470–88.

[5] van der Meel R, Sulheim E, Shi Y, Kiessling F, Mulder WJM, Lammers T. Smart cancer nanomedicine. Nat Nanotechnol. 2019;14(11):1007–17.

[6] Heinhuis KM, Ros W, Kok M, Steeghs N, Beijnen JH, Schellens JHM. Enhancing antitumor response by combining immune checkpoint inhibitors with chemotherapy in solid tumors. Ann Oncol. 2019;30(2):219–35.

[7] Khatibi SA, Misaghi A, Moosavy M-H, Basti AA, Koohi MK, Khosravi P, et al. Encapsulation of Zataria multiflora Bioss. Essential oil into nanoliposomes and *in vitro* antibacterial activity against *Escherichia coli* O157:H7. J Food Process Preservation. 2017;41(3):e12955.

[8] Abtahi NA, Naghib SM, Ghalekohneh SJ, Mohammadpour Z, Nazari H, Mosavi SM, et al. Multifunctional stimuli-responsive niosomal nanoparticles for co-delivery and co-administration of gene and bioactive compound: *In vitro* and *in vivo* studies. Chem Eng J. 2022;429:132090.

[9] Sartipzadeh O, Naghib SM, Shokati F, Rahmanian M, Majidzadeh-A K, Zare Y, et al. Microfluidic-assisted synthesis and modelling of monodispersed magnetic nanocomposites for biomedical applications. Nanotechnol Rev. 2020;9(1):1397–407.

[10] Huang Y, Zeng J. Recent development and applications of nanomaterials for cancer immunotherapy. Nanotechnol Rev. 2020;9(1):367–84.

[11] Kalantari E, Naghib SM. A comparative study on biological properties of novel nanostructured monticellite-based composites with hydroxyapatite bioceramic. Mater Sci Engineering: C. 2019;98:1087–96.

[12] Mirhosseini M, Shekari-Far A, Hakimian F, Haghiralsadat BF, Fatemi SK, Dashtestani F. Core-shell Au@Co-Fe hybrid nanoparticles as peroxidase mimetic nanozyme for antibacterial application. Process Biochem. 2020;95:131–8.

[13] Gooneh-Farahani S, Naimi-Jamal MR, Naghib SM. Stimuli-responsive graphene-incorporated multifunctional chitosan for drug delivery applications: a review. Expert Opin Drug Delivery. 2019;16(1):79–99.

[14] Malekimusavi H, Ghaemi A, Masoudi G, Chogan F, Rashedi H, Yazdian F, et al. Graphene oxide-l-arginine nanogel: A pH-sensitive fluorouracil nanocarrier. Biotechnol Appl Biochem. 2019;66(5):772–80.

[15] Gooneh-Farahani S, Naghib SM, Naimi-Jamal MR, Seyfoori A. A pH-sensitive nanocarrier based on BSA-stabilized graphene-chitosan nanocomposite for sustained and prolonged release of anticancer agents. Sci Rep. 2021;11(1):17404.

[16] Giordano A, Tommonaro G. Curcumin and cancer. Nutrients. 2019;11(10):2376.

[17] Hewlings SJ, Kalman DS. Curcumin: a review of its effects on human health. Foods. 2017;6(10):92.

[18] Griñán-Ferré C, Bellver-Sanchis A, Izquierdo V, Corpas R, Roig-Soriano J, Chillón M, et al. The pleiotropic neuroprotective effects of resveratrol in cognitive decline and Alzheimer's disease pathology: from antioxidant to epigenetic therapy. Ageing Res Rev. 2021;67:101271.

[19] Reiter RJ, Rosales-Corral SA, Tan D-X, Acuna-Castroviejo D, Qin L, Yang S-F, et al. Melatonin, a full service anti-cancer agent: inhibition of initiation, progression and metastasis. Int J Mol Sci. 2017;18(4):843.

[20] Moballegh Nasery M, Abadi B, Poormoghadam D, Zarrabi A, Keyhanvar P, Khanbabaei H, et al. Curcumin delivery mediated by bio-based nanoparticles: a review. Molecules. 2020;25(3):689.

[21] Ge X, Wei M, He S, Yuan W-E. Advances of non-ionic surfactant vesicles (niosomes) and their application in drug delivery. Pharmaceutics. 2019;11(2):55.

[22] Durak S, Esmaeili Rad M, Alp Yetisgin A, Eda Sutova H, Kutlu O, Cetinel S, et al. Niosomal drug delivery systems for ocular disease—recent advances and future prospects. Nanomaterials. 2020;10(6):1191.

[23] Barani M, Mirzaei M, Torkzadeh-Mahani M, Lohrasbi-Nejad A, Nematollahi MH. A new formulation of hydrophobin-coated niosome as a drug carrier to cancer cells. Mater Sci Engineering: C. 2020;113:110975.

[24] Rathee J, Kanwar R, Kaushik D, Salunke DB, Mehta SK. Niosomes as efficient drug delivery modules for encapsulation of Toll-like receptor 7 agonists and IDO-inhibitor. Appl Surf Sci. 2020;505:144078.

[25] Moghddam SRM, Ahad A, Aqil M, Imam SS, Sultana Y. Formulation and optimization of niosomes for topical diacerein delivery using 3-factor, 3-level Box-Behnken design for the management of psoriasis. Mater Sci Eng C. 2016;69:789–97.

[26] Barani M, Nematollahi MH, Zaboli M, Mirzaei M, Torkzadeh-Mahani M, Pardakhty A, et al. In silico and *in vitro* study of magnetic niosomes for gene delivery: The effect of ergosterol and cholesterol. Mater Sci Eng C. 2019;94:234–46.

[27] Zheng M, Pan M, Zhang W, Lin H, Wu S, Lu C, et al. Poly (α-L-lysine)-based nanomaterials for versatile biomedical applications: current advances and perspectives. Bioactive Materials. 2021;6(7):1878–909.

[28] Moghaddam SV, Abedi F, Alizadeh E, Baradaran B, Annabi N, Akbarzadeh A, et al. Lysine-embedded cellulose-based nanosystem for efficient dual-delivery of chemotherapeutics in combination cancer therapy. Carbohydr Polym. 2020;250:116861.

[29] Sharma V, Anandhakumar S, Sasidharan M. Self-degrading niosomes for encapsulation of hydrophilic and hydrophobic drugs: an efficient carrier for cancer multi-drug delivery. Mater Sci Eng C Mater Biol Appl. 2015;56:393–400.
[30] Agarwal Y, Rajinikanth PS, Ranjan S, Tiwari U, Balasubramnaiam J, Pandey P, et al. Curcumin loaded polycaprolactone-/polyvinyl alcohol-silk fibroin based electrospun nanofibrous mat for rapid healing of diabetic wound: an *in vitro* and in-vivo studies. Int J Biol Macromol. 2021;176:376–86.
[31] Kamaly N, Yameen B, Wu J, Farokhzad OC. Degradable controlled-release polymers and polymeric nanoparticles: mechanisms of controlling drug release. Chem Rev. 2016;116(4):2602–63.
[32] Das SS, Bharadwaj P, Bilal M, Barani M, Rahdar A, Taboada P, et al. Stimuli-responsive polymeric nanocarriers for drug delivery, imaging, and theragnosis. Polymers. 2020;12(6):1397.
[33] Cicuéndez M, Doadrio JC, Hernández A, Portolés MT, Izquierdo-Barba I, Vallet-Regí M. Multifunctional pH sensitive 3D scaffolds for treatment and prevention of bone infection. Acta Biomaterialia. 2018;65:450–61.
[34] Cavaliere R, Ciocatto EC, Giovanella BC, Heidelberger C, Johnson RO, Margottini M, et al. Selective heat sensitivity of cancer cells. Biochemical and clinical studies. Cancer. 1967;20(9):1351–81.
[35] Wong KE, Ngai SC, Chan KG, Lee LH, Goh BH, Chuah LH. Curcumin nanoformulations for colorectal cancer: a review. Front Pharmacol. 2019;10:152.
[36] Yallapu MM, Othman SF, Curtis ET, Bauer NA, Chauhan N, Kumar D, et al. Curcumin-loaded magnetic nanoparticles for breast cancer therapeutics and imaging applications. Int J Nanomed. 2012;7:1761–79.
[37] Awasthi R, Kumar S, Kulkarni T. G. Frontier lipid-based carrier systems for drug targeting: a laconic review on niosomes. Pharm Nanotechnol. 2014;2(3):116–28.
[38] Abdelkader H, Alani AWG, Alany RG. Recent advances in non-ionic surfactant vesicles (niosomes): self-assembly, fabrication, characterization, drug delivery applications and limitations. Drug Delivery. 2014;21(2):87–100.
[39] Yeo PL, Lim CL, Chye SM, Ling APK, Koh RY. Niosomes: a review of their structure, properties, methods of preparation, and medical applications. Asian Biomed. 2017;11(4):301–13.
[40] Abbas P, Esmaeil M. Nano-niosomes drug, vaccine gene delivery: a rapid overview. Nanomed J. 2013;1(1):1–2.
[41] Ciani L, Ristori S, Salvati A, Calamai L, Martini G. DOTAP/DOPE and DC-Chol/DOPE lipoplexes for gene delivery: zeta potential measurements and electron spin resonance spectra. Biochimica et Biophysica Acta (BBA) – Biomembranes. 2004;1664(1):70–9.
[42] Simberg D, Weisman S, Talmon Y, Barenholz Y. DOTAP (and other cationic lipids): chemistry, biophysics, and transfection. Crit Reviews™ Therapeutic Drug Carr Syst. 2004;21(4):1–62.
[43] Pun SH, Hoffman AS. B.8 – Nucleic acid delivery. In: Ratner BD, Hoffman AS, Schoen FJ, Lemons JE, editors. Biomaterials science (Third edn.). Cambridge, Massachusetts, USA: Academic Press; 2013. p. 1047–54.
[44] Huang K-Y, Hsu JB-K, Lee T-Y. Characterization and identification of lysine succinylation sites based on deep learning method. Sci Rep. 2019;9(1):1–15.
[45] Mukerjee A, Vishwanatha JK. Formulation, characterization and evaluation of curcumin-loaded PLGA nanospheres for cancer therapy. Anticancer Res. 2009;29(10):3867–75.
[46] Burgos-Morón E, Calderón-Montaño JM, Salvador J, Robles A, López-Lázaro M. The dark side of curcumin. Int J Cancer. 2010;126(7):1771–5.
[47] Tarantino C, Paolella G, Cozzuto L, Minopoli G, Pastore L, Parisi S, et al. miRNA 34a, 100, and 137 modulate differentiation of mouse embryonic stem cells. FASEB J. 2010;24(9):3255–63.
[48] Bansal SS, Goel M, Aqil F, Vadhanam MV, Gupta RC. Advanced drug delivery systems of curcumin for cancer chemoprevention. Cancer Prev Res. 2011;4(8):1158.
[49] Aggarwal BB, Harikumar KB. Potential therapeutic effects of curcumin, the anti-inflammatory agent, against neurodegenerative, cardiovascular, pulmonary, metabolic, autoimmune and neoplastic diseases. Int J Biochem Cell Biol. 2009;41(1):40–59.
[50] Thangapazham RL, Sharma A, Maheshwari RK. Multiple molecular targets in cancer chemoprevention by curcumin. AAPS J. 2006;8(3):E443.